HHS Public Access

Author manuscript

*Matrix Biol*. Author manuscript; available in PMC 2019 April 01.

Published in final edited form as:

*Matrix Biol*. 2018 April ; 67: 15–31. doi:10.1016/j.matbio.2018.02.011.

# Roles of Ihh signaling in chondroprogenitor function in postnatal condylar cartilage

**Naito Kurio**[2,3], **Cheri Saunders**[1], **Till E. Bechtold**[1,4], **Imad Salhab**[2], **Hyun-Duck Nah**[2], **Sayantani Sinha**[1], **Paul C. Billings**[1], **Maurizio Pacifici**[1], and **Eiki Koyama**[1]

[1]Division of Orthopaedic Surgery, Department of Surgery, The Children's Hospital of Philadelphia, Philadelphia, PA 19104

[2]Division of Plastic and Reconstructive Surgery, Department of Surgery, The Children's Hospital of Philadelphia, Philadelphia, PA 19104

[3]Department of Oral and Maxillofacial Surgery, Okayama University Graduate School of Medicine, Okayama, 2-5-1, Japan

[4]Department of Orofacial Orthopaedics, Center of Dentistry and Oral Medicine, University Hospital Tuebingen, D-72076 Tuebingen, Germany

## Abstract

Condylar articular cartilage in mouse temporomandibular joint develops from progenitor cells near the articulating surface that proliferate, undergo chondrogenesis and mature into hypertrophic chondrocytes. However, it remains unclear how these processes are regulated, particularly postnatally. Here we focused on the apical polymorphic layer rich in progenitors and asked whether the phenotype and fate of the cells require signaling by Indian hedgehog (Ihh) previously studied in developing long bones. In condyles in newborn mice, the apical polymorphic/progenitor cell layer was ~10 cell layer-thick and expressed the articular matrix marker *Tenascin-C* (*Tn-C*), and the underlying thick cell layer expressed *Tn-C* as well as the chondrogenic master regulator *Sox9*. By 1 month, condylar cartilage had gained its full width, but became thinner along its main longitudinal axis and displayed hypertrophic chondrocytes. By 3 months, articular cartilage consisted of a 2–3 cell layer-thick zone of superficial cells and chondroprogenitors expressing both

Corresponding author: Eiki Koyama, Division of Orthopaedic Surgery, The Children's Hospital of Philadelphia, 3615 Civic Center Boulevard, ARC Suite 902, Philadelphia, PA 19104, USA, 267-425-2074 (phone), 267-426-7814 (fax), koyamae@email.chop.edu. Current Address: Naito Kurio: Department of Oral Surgery, Tokushima University Graduate School, Tokushima, 3-18-15, Japan

**CONFLIC OF INTEREST:** The authors declare that they have no conflict of interest.

**AUTHOR CONTRIBUTIONS:**

Conception and design: EK
Analysis and Interpretation of the data: NK, CS, TB, IS, SS, HDN
Drafting the Article: EK, PCB
Critical revision of the article for important intellectual content: EK, MP
Final approval of the article: KN, CS, TB, IS, SS, HDN, PCB, MP, EK
Obtaining of funding: EK, HDN
Collection and assembly of data: NK, CS, TB, IS, SS

*Tn-C* and *Sox9* and a bottom zone of chondrocytes displaying vertical matrix septa. EdU cell tracing in juvenile mice revealed that conversion of chondroprogenitors into chondrocytes and hypertrophic chondrocytes required about 48 and 72 hrs, respectively. Notably, EdU injection in 3 month-old mice labeled both progenitors and maturing chondrocytes by 96 hrs. Conditional ablation of *Ihh* in juvenile/early adult mice compromised chondroprogenitor organization and function and led to reduced chondroprogenitor and chondrocyte proliferation. The phenotype of mutant condyles worsened over time as indicated by apoptotic chondrocyte incidence, ectopic chondrocyte hypertrophy, chondrocyte column derangement and subchondral bone deterioration. In micromass cultures of condylar apical cells, hedgehog (Hh) treatment stimulated chondrogenesis and alkaline phosphatase (APase) activity, while treatment with HhAntag inhibited both. Our findings indicate that the chondroprogenitor layer is continuously engaged in condylar growth postnatally and its organization and functioning depend on hedgehog signaling.

### Keywords

TMJ; mandibular condyle; fibrocartilage; Ihh; progenitor cells

## INTRODUCTION

The temporomandibular joint (TMJ) is essential for jaw movement during speech and mastication, and its malfunction can have a major impact on quality of life [1]. The TMJ is composed by the glenoid fossa in the temporal bone, the articular disc and the mandibular condyle. The mandibular condylar cartilage has attracted a great deal of attention from researchers and clinicians owing to its unique biological features and essential roles for proper joint mechanics by providing both tensile and compressive strength, respectively [2, 3]. Articular cartilage constituting other synovial joints in the body is classified as hyaline and exhibits poor repair capacity when damaged [4–7]. In contrast, condylar articular cartilage, which is classified as the same fibrocartilage as knee meniscus and articular disc, exhibits many distinguishing features, including an especially strong adaptive remodeling capacity in response to biomechanical stimulation [8–10].

Developing condylar articular cartilage displays a characteristic stratified organization and consists of: a thin superficial zone composed of flat and tightly-bound cells; a polymorphic (*pm*)/progenitor (*pr*) layer in which chondroprogenitors actively proliferate and produce chondrocytes by appositional growth; and a bottom zone containing flattened/maturing and hypertrophic chondrocytes in which the cells undergo endochondral bone formation [11–13]. Unlike long bones that contain a secondary ossification center at each apical end, condylar cartilage functions both as articular cartilage and growth site. As such, it is characterized by expression of multiple gene products including: *Proteoglycan 4* (*Prg4*) which acts as a joint boundary lubricant both alone and in combination with hyaluronan (HA) [13–17]; *Tenascin-C* (*Tn-C*) which is an articular chondrocyte-associated protein with chondro-protective ability [18–20]; *Collagens type II and type X* (*Col-II and Col-X*), well characterized markers of immature and hypertrophic chondrocytes, respectively; and signaling proteins, transcription factors and extracellular matrix [21–26]. In addition, condylar chondrocytes express *Collagen type I* and the surface of mature condylar cartilage

is lined with a fibrous/superficial tissue, similar to the superficial and polymorphic/chondroprogenitor layer in mice by the histological evaluation, and is prominent in other species such as rat and human, as characterizes fibrocartilaginous features of the condylar cartilage [22, 27, 28]. It is widely recognized that cells with chondroprogenitor characteristics play important roles in not only the structural organization of condylar cartilaginous tissues, but also the cartilage homeostasis which maintain the unique biomechanical function of the structure including remodeling capacities to biomechanical stimuli [8, 9]. A recent study shows that the fibrous tissue of condyles in rats plays a role as a niche that harbors fibrocartilage stem cells [28] [20]. However, our understanding how such cells acquire their chondroprogenitor character and maintain their functions remains far from complete.

Genetic studies in mice have shown that signaling molecules play essential roles in endochondral bone formation during embryonic and postnatal life. Among them, Indian hedgehog (Ihh) signaling regulates a variety of processes during skeletal development, including the growth of long bones and synovial joint formation [29–31]. Phenotypic characterization of global or conditional *Ihh* mouse mutants shows that *Ihh* is required for chondrocyte proliferation and maturation, intramembranous bone formation, joint cavitation and morphogenesis [30, 31]. Similar findings have been reported in the TMJ. Global *Ihh* knockout or conditional ablation of Hh signaling at embryonic stages led to abnormal disc and synovial cavity formation and condylar cartilage dysplasia [21]. Inactivation or modulation of Ihh signaling in cartilage at birth resulted in condylar cartilage growth retardation and disc fusion [32–35]. While these data clearly demonstrate pivotal roles for Ihh in TMJ development during embryonic and early postnatal stages, the roles of Ihh signaling in chondroprogenitor function at juvenile and adult stages have not been fully clarified.

In the present study, we investigated the cellular organization of the polymorphic/progenitor layer, chondroprogenitor cell fate and function, and possible role(s) of Ihh signaling in these processes. Condylar cartilage displays dynamic structural changes in the polymorphic/progenitor layer during postnatal growth. EdU-progenitor tracing analyses in juvenile and adult mice reveals that EdU-labeled chondroprogenitor cells give rise to mature chondrocytes, where such processes become less frequent and take longer in adult mice. We also find that in conditional $Ihh^{f/f};Aggrecan^{tm(IRES\text{-}creERT2)}$ (hereafter $Ihh^{f/f};Agc\text{-}CreER$) knockout (KO) mice, loss of Ihh signaling diminishes the ability of progenitors to proliferation and undergo chondrogenesis. Finally, treatment of primary condylar apical cells with recombinant human Sonic hedgehog protein (rhSHH) promotes chondrogenesis and chondrocyte maturation, while inhibition of Hedgehog (Hh) signaling attenuates basal chondrogenesis. Thus, our studies indicate that proper functioning of chondroprogenitor cells in condylar cartilage during postnatal life is exquisitely sensitive to hedgehog signaling.

## 2. Results

### 2.1. Development of polymorphic/progenitor layer and structure of condylar articular cartilage during postnatal development

To clarify means by which chondroprogenitor cells in condylar articular cartilage develop and reach structural and functional maturity over time, we closely examined condylar cartilage in mice ranging from newborn to 3 months of age. In neonates, the medio-lateral width of articular cartilage was about 180 μm and thus relatively narrow; by 1 month, it became almost 3 times wider and remained so thereafter (Figs. 1A, 1H, 1O). Articular cartilage longitudinal thickness was about 470μm at newborn stages, decreased to about 120 μm by 1 month and remained such through adulthood (Figs. 1V). The polymorphic/progenitor (*pr*) layer, which is distinguishable from the underlying cartilage matrix-rich chondrocytes by SafraninO/fast-green staining, was about 60 μm thick in newborns and consisted of an average of 17 cell layers; it became about 12 μm thick by 1 month and decreased further by 3 months, displaying an average 6 μm thickness and 2–3 cell layers (Figs. 1B, 1I, 1P, 1W. 1X). To characterize the cellular phenotypes in the cell layer and articular cartilage we carried out *in situ* hybridization. In newborn condyles, *Tn-C* transcripts were present at the apical end and characterized the progenitor cell layer but less so the superficial (*sf*) cells (Figs. 1B–1C). Transcripts for *Col-II*, a typical chondrocyte marker (Fig. 1E), were not detectable in either cell population. Transcripts for *Sox9*, a master gene for chondrogenesis, were only detected in cells at the bottom half of the progenitor layer (Figs. 1D). These expression patterns in the progenitor layer were maintained in juvenile and adult stages (Figs. 1J–1K, 1Q), except for *Tn-C* and *Sox-9* expression that became detectable in both superficial cells and choondroprogenitors by adult stages (Figs. 1Q–1R). Immature chondrocytes in the flattened cell layer (*fl*) expressed *Col-II* (Figs. 1E, 1L, 1S), and hypertrophic chondrocytes began to express *Col-X* (Figs. 1M, 1T). Notably, large chondrocytes 25–30 μm in diameter emerged during juvenile stages (Figs. 1I, arrowheads; 1Y) while condylar articular cartilage exhibited rapid lateral expansion. However, by 3 months, these large chondrocytes were no longer detectable (Figs. 1P, 1Y), and resident chondrocytes were organized in columns (Fig. 1P, arrowheads) separated by longitudinal cartilage matrix septa, which were not recognizable at earlier stages (Figs. 1G, 1N, 1U, arrowheads, respectively). Subchondral bone plate (*sb*) was fully formed by these stages, supporting articular cartilage (Fig. 1O, arrowheads).

### 2.2. Mapping of chondroprogenitors and their fate in postnatal condylar articular cartilage

To further address chondroprogenitors' fate in postnatal condylar articular cartilage, we performed EdU labeling and tracing analyses. Mice were injected with EdU at 2 weeks of age, and 4 hr prior to being sacrificed at indicated time points. EdU-labeled cells in condylar cartilage tissues were mainly localized in the progenitor layer by 24 hr after the initial EdU injection (Fig. 2A–2B), and continuously detected until 96 hr (Fig. 2C–2E, 2K). Some EdU-labeled chondroprogenitor cells differentiated into chondrocytes and became dispersed into the underlying flattened chondrocyte layer (*fl*) by 48 hr (Fig. 2C). These cells were detectable in the hypertrophic zone (*hl*) by 72 hr (Fig. 2D, 2L, arrowheads) and became more abundant at later time points (Fig. 2E, 2L, arrowheads). Compared to condylar cartilage, tibial growth plate revealed that while EdU-labeled chondrocytes were consistently

detected in the proliferating zone (*pl*) of growth plate from 24 hr to 96 hr (Figs. 2F–2J, 2M), EdU-labeled cells became detectable in hypertrophic zone (*hz*) as early as by 48 hr after the initial EdU injection (Fig. 2H, 2N, arrowheads) and the EdU-labeled chondrocytes exhibited a clear column organization (Figs. 2I, 2J, arrowheads). We next investigated chondroprogenitors' fate of condylar articular cartilage in adult mice by EdU injection at 3 months. Compared to younger mice, fewer EdU-labeled chondroprogenitors were observed (Fig. 2R), but were still detectable at the superficial/progenitor layers (*sf/pr*) of the condylar apical end (Figs. 2Q, 2R). Importantly, EdU-positive progeny cells were present in the underlying chondrocyte zones (*ch*) by 96 hr (Figs. 2O–2R, arrowheads).

### 2.3. Evaluation of specificity of Cre recombinase activity in postnatal TMJs of *Agc-CreERT2;R26-tdTomato* reporter mice

To determine whether hedgehog signaling regulates the cellular organization of the progenitor layer and chondroprogenitor cell fate and function, we employed a genetic approach, using *floxed Ihh* mice mated with transgenic *Agc-CreER* mice in which transgene expression in cartilage of cranial face and appendicular skeleton persists through postnatal life [36, 37]. To make sure that the *Cre* line could induce gene recombination in fibrocartilaginous tissues in TMJs, we initially produced *Agc-CreER;R26-tdTomato* reporter mice injected with tamoxifen once at P14. Two days after tamoxifen injection, reporter activity became detectable throughout the bulk of cartilaginous tissues in glenoid fossa (*gf*) and condyle (*co*), including chondroprogenitors and chondrocytes; however, there were few, if any, reporter-positive cells in articular disc (*dc*), retrodiscal tissue (*rd*) and cells in marrow cavities (Figs. 3A–3B). By 4 weeks after tamoxifen injection, most of cells in articular cartilage were still reporter positive, but there were also clusters of reporter-negative progenitors and chondrocytes in the posterior regions of condylar cartilage (Figs. 3E–3H, arrowheads), implying that those progenitors and their progeny had not undergone recombination. Interestingly, a large number of marrow cells became reporter positive (Figs. 3F, 3H, double arrowhead). There was no detectable reporter activity in companion *Agc-CreER;R26-tdTomato* reporter mice injected with vehicle (Fig. 3C–3D), confirming the non-leakiness of Cre-recombinase activity.

### 2.4. Analysis of hedgehog signaling in postnatal TMJs in *Agc-CreER;Ihh $^{f/f}$;Gli1-nLacZ* mice

To clarify the extent to which hedgehog signaling was affected in *Agr-CreER;Ihh $^{f/f}$* mice, we generated triple transgenic mice by crossing *Agr-CreER;Ihh $^{f/f}$* mice with *Gli1-nLacZ* reporter mice which harbor a β-galactosidase knock-in mutation and are used as a real time read-out of endogenous hedgehog signaling in responding cells in embryonic and postnatal mice [33, 38]. Triple mutant mice received a single injection of tamoxifen or vehicle at P14. Whole mount LacZ staining in TMJ tissues dissected out 2 days post-injection showed that LacZ-positive cells covered the entire surface of control condyles (Figs. 3I, 3J); however, LacZ-positive cells were significantly decreased in condylar articular cartilage (*co*) from tamoxifen-treated mutant mice (Figs. 3K, 3L, arrow), except for cells residing at the anterior and posterior ends of condylar cartilage (Figs. 3K, 3L, arrowheads). Decreased Hh signaling was also observed in the articular cartilage of mutant glenoid fossa (*gf*) compared to controls (Figs. 3M–3P, respectively),

### 2.5. Disruption of chondroprogenitor function and zonal organization in TMJs of *Agc-CreER;Ihh* $^{f/f}$ mice

We next investigated the roles of Ihh signaling in chondroprogenitor function and zonal organization of condylar articular cartilage in juvenile and adult mice. Compound *Agc-CreER;Ihh*$^{f/f}$*;Gli1-nLacZ* and control (*Ihh*$^{f/f}$*;Gli1-nLacZ*) mice received tamoxifen at P14, P21 and P 28, and mice were harvested at 6 weeks of age. Control condylar cartilage displayed a well-organized zone organization as indicated by *Ihh* expression in prehypertrophic/hypertrophic chondrocytes (Figs. 4A, 4C, right panel). LacZ-positive cells were detected in the superficial/progenitor layer as well as chondrocytes (Fig. 4C, left panel), indicating that Ihh diffuses away from chondrocytes toward the condylar apical region, as has been shown in early postnatal condyles [33]. In sharp contrast, the central region along the anterior-posterior axis of mutant condyles became abnormal, displaying decreased numbers of chondroprogenitors and chondrocytes (Figs. 4B, *cp, ch*, bracket, respectively) compared to controls, in which small round chondrocytes were present throughout articular cartilage (Fig. 4B, arrowhead). As expected, *LacZ*-positive cells were not detectable in the condyles (Fig. 4D). We next analyzed the regulatory roles of Hh signaling in cell proliferation and apoptosis. Immunohistochemistry for Ki67 revealed that while a substantial number of chondroprogenitors in control condyles were proliferating, there was a significant reduction of proliferating cells in mutant condyles by 6 weeks (Figs. 4E, 4F, arrowhead, 4K, $p<0.0001$), and such cells became even fewer by 14 weeks (Figs. 4G, 4H, arrowhead, 4K, $p<0.0001$). On the other hand, TUNEL-positive apoptotic cells were more abundant in mutant cartilage by 14 weeks compared to controls (Figs. 4I, 4J, arrowheads, 4L, $p=0.015$). Condylar articular cartilage from 14 week-old mutants also exhibited a significant loss of superficial and chondroprogenitor cells, accompanied by decreased expression of *Sox9* in chondroprogenitors compared to controls (Figs. 5A–5B, double arrowhead; 5C–5D, arrowhead, respectively). Notably, ectopic hypertrophic chondrocytes emerged near the articular surface (Fig. 5B), expressed *Col-X* and *Mmp-13* (Figs. 5G, 5H, arrowhead, respectively), and underwent clustering (Fig. 5B, arrowhead). By 5 months, μCT analyses showed that the central portions of mutant condyles manifested degenerative changes such as irregular and porous subchondral bone compared to controls (Figs. 5I, 5J, respectively), thereby decreasing bone volume fraction and increasing trabecular spacing (Figs. 5M, $p=0.002$; 5N, $p=0.0015$, respectively). Histological inspection further confirmed the presence of abnormal subchondral bone compared to controls (Figs. 5K, 5L, respectively).

### 2.6. Hh signaling promotes chondrogenesis and chondrocyte maturation in condylar apical cell culture

Data above indicate that ablation of Hh signaling severely compromises the progenitor layer organization, chondrogenesis and chondrocyte maturation in condylar cartilaginous tissues. To more directly analyze Hh signaling roles in chondrogenesis, we tested the responses of condylar-derived primary cells to Hh treatment. Condylar apical cell cultures were prepared using a cell isolation method, whereby sequential digestion (i.e. 0.25% trypsin followed by 0.1U collagenase for 5 min per each digestion) of P7 mouse condyles cleanly removes apical cells from the rest of the structure (Figs. 6A, 6B). Apical cells exhibited a characteristic pattern of gene expression including superficial and chondrogenic markers such as *Sox9* as

well as Hh receptors, *Ptc* and *Smo*, thus displaying an expression prolife distinct from that of articular disc cells. Condylar apical cells were reared in high-density micromass cultures. Treatment of these cultures with recombinant human SHH (rhSHH) resulted in a dose-dependent increase of alcian blue-stainable proteoglycan matrix (Fig. 6D) compared to controls. Treatment with rhSHH significantly increased alkaline phosphatase (APase) activity in a dose dependent manner by day 7 compared to controls while HhAntag, a hedgehog signaling inhibitor, significantly attenuated APase activity. Moreover, HhAntag treatment attenuated rhSHH-induced APase activity as well.

## 3. Discussion

Our data show that condylar cartilage displays characteristic arrangements of chondroprogenitor cells and chondrocytes with distinct size and phenotype at successive postnatal stages and in particular, that Ihh signaling play important roles in maintaining the character and function of chondroprogenitor cells. At newborn stages, the polymorphic/progenitor layer is conspicuous and consists of cells with distinctive features, characterized by the presence of *Tn-C*-positive/*Sox9*-negative cells residing in the upper half and *Tn-C* positive/*Sox9*-expressing chondroprogenitors residing in the lower half (Fig. 7A). As the condyle grows rapidly, *Tn-C*-positive/*Sox9*-negative cells become fewer and are no longer detectable in adults (Figs. 7B–7C). These data suggest that these cell populations may serve as a pool of chondroprogenitor cells during postnatal development and growth of condylar articular cartilage. What is the prospective function of *Tn-C* positive/*Sox9*-expressing cells residing at the apical end of the adult condylar cartilage? Our fate mapping analysis of condyles in 3-month-old mice reveals that EdU-labeled cells continue to undergo chondrogenesis and to provide chondrocytes to the condylar cartilage. Thus, we conclude that *Tn-C* positive/*Sox9*-expressing cells possess a chondroprogenitor-like character and replenish chondrocytes in condylar cartilage in juvenile/adult stages. Such *Tn-C* positive/*Sox9*-expressing cells may play a role during times when condylar tissues undergo adaptive remodeling in response to biomechanical stimuli at juvenile/adult stages.

Our data show that conditional ablation of Ihh signaling in condylar cartilage is associated with severe derangement of the polymorphic/progenitor layer organization, accompanied by a significant decrease in chondroprogenitor proliferation and *Tn-C/Sox9*-expressing cells in this layer (Fig. 7. D–E). We also show that in primary condylar apical cell cultures, treatment with rhSHH promotes chondrogenesis and APase activity while a selective Hh signaling inhibitor, Hh Antag, blocks rhSHH actions. Thus, our results strongly suggest that Ihh signaling plays roles in maintaining the character and functions of chondroprogenitor cells in juvenile/adult condylar cartilage. In our previous studies in which we characterized TMJs in *Col2a1-CreER;Ihh*$^{f/f}$, we reported loss of chondrocyte topographical arrangement in condylar cartilage in early postnatal mice. In the present study, we utilized *Agr-CreER* mouse line to ablate Ihh expression in maturing chondrocytes owing to its Cre-recombinase expression and action in chondrocytes even at juvenile/adult stages [36, 37]. In compound *Agr-CreER;Ihh*$^{f/f}$*;Gli1-nLacZ* mice, we document the specificity of induced Cre activity and subsequent depletion of Ihh signaling in articular cartilage of the condyle and glenoid fossa. Utilizing this approach, we observe severe cellular derangements at early stages, and also find progressive degenerative changes affecting the function of chondroprogenitor cells as

well as the derangement of articular subchondral bone plate. Thus, the current study supports and further extends our previous work and demonstrate, for the first time, that Hh signaling plays a vital role in condylar articular cartilage growth in adult animals.

Mandibular condylar chondrocytes exhibit rapid hypertrophy during early condylar cartilage development [22] as indicated by expression of *collagen type X* (a marker for hypertrophic chondrocytes) along with collagens *type I* and *type II* (markers for immature condylar chondrocytes). However, the time frame of chondrogenesis and chondrocyte maturation had not been elucidated in the condylar cartilage of juvenile/adult mice. Our EdU-labeling and tracking analyses in condylar articular cartilage of 2-week-old mice show that the conversion of chondroprogenitor cells into immature chondrocytes takes approximately 24 hr and the successive conversion of progenitors into hypertrophic chondrocytes takes place by approximately 72 hr after initial EdU injection. In tibial growth plate, while many EdU-labeled chondrocytes remain in the proliferative zone, the EdU-labeled chondrocytes leave the zone and become detectable in the hypertrophic zone by 48 hr, which is consistent with previous results [39]. Therefore, these findings suggest that newly differentiated chondrocytes in juvenile condylar cartilage undergo hypertrophy over a similar time frame as those in tibial growth plate, even though the overall amount of growth achieved is different at each site.

In this study, we employed *Agc-CreER* mice to ablate *Ihh* in fibrocartilage of TMJs. We find very specific reporter activation in articular cartilage of glenoid fossa and condyle, but not in non-cartilaginous tissues including articular disc, retrodiscal tissue and lateral pterygoid muscle. Using compound *Agc-CreER;Ihh*$^{f/f}$*;Gli1-nLacZ* mice, we observe decreased numbers of LacZ-positive chondroprogenitors and chondrocytes in TMJ articular cartilage, providing evidence that *Agr-CreER*-mediated recombination is efficient and highly specific. In condylar cartilage, a small number of LacZ-positive cells is observed at the anterior and posterior ends of condylar cartilage, likely reflecting characteristic *Aggrecan* promoter-mediated Cre recombination in TMJs. Further studies will be needed to assess how these cell populations evade Cre-recombination and/or where these cells emerge over time. A similar observation on Cre recombination in condylar cartilage using *Agc-CreER* line has been reported previously [40].

The results of the current study provide insights into the relationship between Ihh gene expression and its target cells in the juvenile/adult condylar articular cartilage. It is clear from our results in compound mutant *Agr-CreER;Ihh*$^{f/f}$*;Gli1-nLacZ* and control *Gli1-nLacZ* mice that IHH produced by prehypertrophic/hypertrophic chondrocytes is able to reach immature chondrocytes as well as progenitor cells residing in the condylar apical region; when *Ihh* is ablated, the functioning of the cells is deranged. IHH was originally proposed to serve as an inhibitor of chondrocyte maturation along with PTHrP expressing periarticular tissues in developing long bones [41, 42]. However, subsequent genetic studies in mice found that IHH signaling actually promotes chondrocyte maturation [43, 44]. Consistent with this idea, in *Ihh*-mutant condylar cartilage, the condylar tissues initially display decreased hypertrophic chondrocytes and relatively small chondrocyte, distributed sparsely in the cartilage, clearly indicating that newly produced chondrocytes fail to undergo maturation. Our in vitro data, using condylar apical cells in culture suggest that Hh signaling

is able to directly regulate chondrocyte maturation. Chondrocytes in *Ihh*-mutant condyles display ectopic hypertrophic chondrocytes expressing *MMP13,* which reside at the apical region near the condylar surface, suggesting that those cells eventually undergo hypertrophic differentiation, but may induce such degenerative changes in the condylar cartilage as found at successive stages. This begs the question, how does IHH reach the apical cells of the condylar cartilage? Studies indicate that IHH proteins are subject to lipid tail modification and subsequently form multimetric micelle-like structures [45, 46]. Hh proteins are also associated with the cell surface by interaction with heparan sulfate proteoglycans (HSPGs) through their intrinsic heparan sulfate/heparin-binding domains (Cardin-Weintraub motif) present in the mature ligand [47–49]. Thus, HSPGs regulate the distribution and action of Hh proteins on target cells and tissues [47, 50]. Further studies should clarify whether biological activity of IHH produced by condylar chondrocytes is regulated by HSPGs in the matrix of condylar cartilage.

## 4. MATERIALS & METHODS

### 4.1. Ethics statement regarding mouse studies

All experiments involving wild-type and transgenic mice were reviewed and approved by the IACUC at The Children's Hospital of Philadelphia (protocol no. IAC 17-001138, principal investigator EK). All animals were handled, treated, and cared for according to the approved protocols and procedures.

### 4.2. Transgenic mouse lines, husbandry and drug treatment

*Ihh* $^{f/f}$ mice (Jackson Labs)[31] and *Aggrecan-CreERT2* (abbreviated to *Agr-CreER*) mice (Jackson Labs)[36] were described previously. *Ihh* $^{f/f}$ mice were mated with *Aggrecan-CreER* mice, expressing *Cre* recombinase linked to a modified estrogen ligand binding domain under the control of *aggrecan* promoter/enhancer sequence, generating compound *Agr-CreER; Ihh* $^{f/f}$ mice. Companion control mice included *Agr-CreER* or *Agr-CreER; Ihh* $^{f/+}$. Control and compound transgenic mice were given multiple intraperitoneal injections of tamoxifen, stock tamoxifen solution was 20 mg/ml in ethanol: corn oil mixture at 1 : 4 ratio (1mg/13 g body weight) at P14, P21 and P28. Mice were sacrificed at indicated time points, and body parts and tissues were processed for imaging and other procedures as described below. To monitor topography of *CreER* action, *Agr-CreER* mice were mated with *R26-tdTomato* reporter mice (Jackson Labs). Compound *Agr-CreER; R26-tdTomato* mice at P14 received a single IP injection of tamoxifen (n=6) or a similar volume of vehicle (ethanol/corn oil) (n=5). Mice were sacrificed at indicated time points, and decalcified for 14 days in 10% EDTA/2% PFA, and 10 μm frozen sections of TMJ samples were processed for imaging. To evaluate the extent of hedgehog signaling inactivation, *Gli1-nLacZ* reporter mice (Jackson labs) [25] were mated with *Agr-CreER; Ihh* $^{f/f}$ mice to generate *Agr-CreER; Ihh* $^{f/f}$*;Gli1-nLacZ* mice. Compound *Agr-CreER; Ihh* $^{f/f}$*;Gli1-nLacZ* mice received either a single IP injection of tamoxifen or a similar volume of vehicle at P14 (n=5/each condition), or multiple IP injections at P14, 21 and 28 to augment Ihh signaling inactivation. Mice were sacrificed at indicated time points, and TMJ samples were processed for β-galactosidase staining (see below).

### 4.3. Histological and immunohistochemical analyses

TMJs from wild-type mice were evaluated at postnatal day 0 (P0), 1 month (1mo) and 3 months (3mos) of age. Images from haematoxylin and eosin stained section were analyzed by histomorphometry with ImagePro 4.5 (Leeds Precision Instruments, Minneapolis, MN, USA). *Agr-CreER; Ihh* $^{f/f}$ and control littermates were evaluated at age of 6 weeks (n=6 mutants and n=5 controls), 14 weeks (n=11 mutants and n=5 controls) and 5 months (n=7 mutants and n=6 controls). Mice were fixed with 4% paraformaldehyde (PFA)/1xPBS overnight, decalcified for 14 days in 10% EDTA/2% PFA/1xPBS, dehydrated, and embedded in paraffin. For histological examination, 5 μm serial sections were processed for hematoxylin/eosin or Safranin-O/fast green staining. Ki67 immunohistochemistry was performed on 5 μm paraffin sections. Antigen retrieval was performed in 10 mM citrate buffer (pH 6.0) at 60°C overnight, followed by incubation at room temperature for 20 min. Endogenous peroxidase activity was blocked by incubation with 3% $H_2O_2$ for 10 min. Sections were treated with goat serum and subsequently incubated with Ki67 primary antibodies (Abcam ab16667, 1:100). After overnight incubation at 4°C, slides were washed in 1xPBS and incubated with biotinylated secondary antibodies at room temperature for 30 min. Finally, slides were incubated with VECTASTAIN ABC reagent for 30 min and the signal was visualized using peroxidase substrates according to the manufacturer's instructions (VECTOR LABORATORIES, Burlingame, CA). Edu (5-ethynyl-2′-deoxyuridine; Life technology A1004) (100mg/kg body weight) was administrated intraperitoneally to mice at P14 or 3 month and 4 hr before sacrifice at each time point. Eight TMJs and eight knee samples from individual mice were analyzed (n=8). Click-iT EdU AlexaFluor imaging kit reaction (Invitrogen, Carlsbad, CA) was used according to manufacturer's protocol, and sections were mounted with Fluoro-Gel II Mounting Medium. Apoptosis detection was carried out on paraffin sections using a TUNEL Assay Kit using manufacturer's instructions (Roche, Mannheim, Germany).

### 4.4. Whole mount β-galactosidase staining

Whole mount β-galactosidase staining of mouse TMJ samples was performed using standard protocols. Briefly, TMJ samples were fixed for 20 min in whole-mount fixative (BG5C; Millipore) on ice. Samples were further dissected out into condyles, discs and glenoid fossae, and processed for X-gal staining for 3–4 hr at 37°C in the dark, post-fixed in 4% PFA/1xPBS at 4°C, and photographed. Glenoid fossae and condyles were decalcified with formic acid, dehydrated, embedded in paraffin, and sectioned at 10μm-thickness.

### 4.5. Cell culture

Cultures were prepared from condylar samples isolated from day 10-old wild-type mice (n=30) as described (Bechtold et al., 2015) with some modifications. Isolated glenoid fossae were incubated with 2.5 U/ml dispase (MP Biomedicals, LLC, Solon, OH) and 600 U/ml (3mg/ml) type I collagenase (Worthington Biochemical Corporation, Lakewood, NJ) in HBSS with $Ca^{2+}$ and $Mg^{2+}$ for 5–10 min at 37°C with gentle agitation. Dissociated cells and tissue fragments were cultured together on collagen 1 substrate-coated 6 well culture plates in DMEM containing 10% FBS, 0.1% Fungizone and antibiotics. Cells were passaged three or four times prior to use in experiment, and processed for micromass culture. Micromass

cultures were initiated by spotting 15 μl of the cell suspensions ($1\times10^6$ cells) onto the collagen 1 substrate in 24-well tissue culture plates. The cultures were grown in DMEM containing 2% FBS and supplemented with recombinant human SHH (rhSHH) (R&D Systems; Minneapolis MN) at a concentration of 125 or 250 ng/ml, HhAntag at a concentration of 2.0 or 5.0 nM, a hedgehog signaling inhibitor that blocks the activity of the signaling receptor Smoothened (provided as a generous gift from Genentech; San Francisco, CA), or a combination of rhSHH/HhAntag. Day 7 cultures were fixed and stained with Alcian blue (pH 1.0). For ALP staining, cultures were washed three times with TBS, then treated with a solution of 5-bromo-4-chloro-3-indolyl-phosphate and nitro blue tetrazolium (Wako Pure Chemical Industries, Ltd.) for 15 min. The integrated density of Alcian blue-stained cultures or ALP-stained cultures were semiquantified using ImageJ.

### 4.6. μCT analysis

Mouse condyles from control (n=6) and mutant (n=6) mice at 5 months of age were examined using a viva μCT 40 CT scanner (Scanco Medical AG, Bruttisellen, Switzerland), and analyzed using μCT v6.0 vivaCT software. Serial 12.5 μm 2-D and 3-D images were acquired at 70 kV and 113 mA. The raw data from the μCT scans were compiled into 2D gray scale images that were then contoured to define the condyles. Binary images were generated using a threshold of 280. Virtual 3D models were then constructed and analyzed for morphological abnormalities.

### 4.7. *In situ* hybridization analyses

For *in situ* hybridization, sections were hybridized with antisense or sense $^{35}$S-labeled riboprobes as described in detail previously[51]. cDNA clones used as templates for probes included: *Sox9* (nt, 116-856; NM_011448), *Tenascin-C* (*Tn-C*) (nt. 151-741; NM_011607); *Collagen II* (*Col II*) (nt.1095-1344; X57982), *Collagen X* (*Col X*) (nt.1302-1816; NM009925), Indian hedgehog (Ihh) (nt. 897-1954; MN_010544) and *Mmp13* (nt. 11-744; BC125320).

### 4.8. Statistical analysis

Data points, averages and 95% confidence intervals are presented in the scatter plots. For histomorphometric analyses, each data point in the scatter plots represents the average value obtained from three to five histological sections/TMJ, and 10 TMJ samples were analyzed/each time point (n=10). For EdU labeling and tracing analyses in TMJs and tibial growth plates, each data point represents the average value obtained from three to five histological sections/TMJ and tibial growth plate, and 10 of TMJs and tibia samples were analyzed/each time point (n=10). For immunohistological and TUNEL analyses, each data point represents the average value obtained from three to five histological sections/TMJ, and eight TMJ samples from *Ihh*-mutant or control mice were analyzed/each time point (n=8). Normality of distribution was confirmed via the Shapiro-Wilk test using Prism 6 GraphPad Software. Statistical significance of differences among averages was determined via unpaired Student's *t*-test using Prism 6 GraphPad Software. Resulting two-tailed $p$-value$< 0.05$ was regarded as statistically significant difference.

## Acknowledgments

This study was supported by NIDCR grant (RO1DE023841 to EK and H-DN). We express our gratitude to the Penn Center for Musculoskeletal Disorders (PCMD) supported by the NIHP30 grant AR069619 where the mouse μCT scans were performed, analyzed and quantified. The authors declare no potential conflicts of interest with respect to the authorship and/or publication of this article.

## REFELENCES

1. Ohrbach R, Dworkin SF. The Evolution of TMD Diagnosis: Past, Present, Future. J Dent Res. 2016; 95(10):1093–101. [PubMed: 27313164]
2. Ruggiero L, Zimmerman BK, Park M, Han L, Wang L, Burris DL, Lu XL. Roles of the Fibrous Superficial Zone in the Mechanical Behavior of TMJ Condylar Cartilage. Ann Biomed Eng. 2015; 43(11):2652–62. [PubMed: 25893511]
3. Chandrasekaran P, Doyran B, Li Q, Han B, Bechtold TE, Koyama E, Lu XL, Han L. Biomechanical properties of murine TMJ articular disc and condyle cartilage via AFM-nanoindentation. J Biomech. 2017; 60:134–141. [PubMed: 28688538]
4. Makris EA, Gomoll AH, Malizos KN, Hu JC, Athanasiou KA. Repair and tissue engineering techniques for articular cartilage. Nat Rev Rheumatol. 2015; 11(1):21–34. [PubMed: 25247412]
5. Decker RS, Koyama E, Pacifici M. Genesis and morphogenesis of limb synovial joints and articular cartilage. Matrix Biol. 2014; 39:5–10. [PubMed: 25172830]
6. Decker RS, Um HB, Dyment NA, Cottingham N, Usami Y, Enomoto-Iwamoto M, Kronenberg MS, Maye P, Rowe DW, Koyama E, Pacifici M. Cell origin, volume and arrangement are drivers of articular cartilage formation, morphogenesis and response to injury in mouse limbs. Dev Biol. 2017; 426(1):56–68. [PubMed: 28438606]
7. Wilusz RE, Sanchez-Adams J, Guilak F. The structure and function of the pericellular matrix of articular cartilage. Matrix Biol. 2014; 39:25–32. [PubMed: 25172825]
8. Shen G, Darendeliler MA. The adaptive remodeling of condylar cartilage---a transition from chondrogenesis to osteogenesis. J Dent Res. 2005; 84(8):691–9. [PubMed: 16040724]
9. Kuroda S, Tanimoto K, Izawa T, Fujihara S, Koolstra JH, Tanaka E. Biomechanical and biochemical characteristics of the mandibular condylar cartilage. Osteoarthritis Cartilage. 2009; 17(11):1408–15. [PubMed: 19477310]
10. Detamore MS, Orfanos JG, Almarza AJ, French MM, Wong ME, Athanasiou KA. Quantitative analysis and comparative regional investigation of the extracellular matrix of the porcine temporomandibular joint disc. Matrix Biol. 2005; 24(1):45–57. [PubMed: 15749001]
11. Wadhwa S, Kapila S. TMJ disorders: future innovations in diagnostics and therapeutics. J Dent Educ. 2008; 72(8):930–47. [PubMed: 18676802]
12. Luder HU, Leblond CP, von der Mark K. Cellular stages in cartilage formation as revealed by morphometry, radioautography and type II collagen immunostaining of the mandibular condyle from weanling rats. Am J Anat. 1988; 182(3):197–214. [PubMed: 3213819]
13. Koyama E, Saunders C, Salhab I, Decker RS, Chen I, Um H, Pacifici M, Nah HD. Lubricin is Required for the Structural Integrity and Post-natal Maintenance of TMJ. J Dent Res. 2014; 93(7): 663–70. [PubMed: 24834922]
14. Jay GD, Waller KA. The biology of lubricin: near frictionless joint motion. Matrix Biol. 2014; 39:17–24. [PubMed: 25172828]
15. Kwiecinski JJ, Dorosz SG, Ludwig TE, Abubacker S, Cowman MK, Schmidt TA. The effect of molecular weight on hyaluronan's cartilage boundary lubricating ability--alone and in combination with proteoglycan 4. Osteoarthritis Cartilage. 2011; 19(11):1356–62. [PubMed: 21872669]
16. Bechtold TE, Saunders C, Decker RS, Um HB, Cottingham N, Salhab I, Kurio N, Billings PC, Pacifici M, Nah HD, Koyama E. Osteophyte formation and matrix mineralization in a TMJ osteoarthritis mouse model are associated with ectopic hedgehog signaling. Matrix Biol. 2016; 52–54:339–354.

17. Bechtold TE, Saunders C, Mundy C, Um H, Decker RS, Salhab I, Kurio N, Billings PC, Pacifici M, Nah HD, Koyama E. Excess BMP Signaling in Heterotopic Cartilage Forming in Prg4-null TMJ Discs. J Dent Res. 2016; 95(3):292–301. [PubMed: 26534931]
18. Ikemura S, Hasegawa M, Iino T, Miyamoto K, Imanaka-Yoshida K, Yoshida T, Sudo A. Effect of tenascin-C on the repair of full-thickness osteochondral defects of articular cartilage in rabbits. J Orthop Res. 2015; 33(4):563–71. [PubMed: 25428773]
19. Okamura N, Hasegawa M, Nakoshi Y, Iino T, Sudo A, Imanaka-Yoshida K, Yoshida T, Uchida A. Deficiency of tenascin-C delays articular cartilage repair in mice. Osteoarthritis Cartilage. 2010; 18(6):839–48. [PubMed: 19747998]
20. Pacifici M. Tenascin-C and the development of articular cartilage. Matrix Biol. 1995; 14(9):689–98. [PubMed: 8785583]
21. Shibukawa Y, Young B, Wu C, Yamada S, Long F, Pacifici M, Koyama E. Temporomandibular joint formation and condyle growth require Indian hedgehog signaling. Dev Dyn. 2007; 236(2): 426–34. [PubMed: 17191253]
22. Fukada K, Shibata S, Suzuki S, Ohya K, Kuroda T. In situ hybridisation study of type I, II, X collagens and aggrecan mRNas in the developing condylar cartilage of fetal mouse mandible. J Anat. 1999; 195(Pt 3):321–9. [PubMed: 10580848]
23. Hinton RJ, Jing J, Feng JQ. Genetic Influences on Temporomandibular Joint Development and Growth. Curr Top Dev Biol. 2015; 115:85–109. [PubMed: 26589922]
24. Yasuda T, Nah HD, Laurita J, Kinumatsu T, Shibukawa Y, Shibutani T, Minugh-Purvis N, Pacifici M, Koyama E. Muenke syndrome mutation, FgfR3P(2)(4)(4)R, causes TMJ defects. J Dent Res. 2012; 91(7):683–9. [PubMed: 22622662]
25. Shirakura M, Kram V, Robinson J, Sikka S, Kilts TM, Wadhwa S, Young MF. Extracellular Matrix Mediates BMP-2 in a Model of Temporomandibular Joint Osteoarthritis. Cells Tissues Organs. 2017; 204(2):84–92. [PubMed: 28419987]
26. Wang Y, Li Y, Khabut A, Chubinskaya S, Grodzinsky AJ, Onnerfjord P. Quantitative proteomics analysis of cartilage response to mechanical injury and cytokine treatment. Matrix Biol. 2017; 63:11–22. [PubMed: 27988350]
27. Visnapuu V, Peltomaki T, Saamanen AM, Ronning O. Collagen I and II mRNA distribution in the rat temporomandibular joint region during growth. J Craniofac Genet Dev Biol. 2000; 20(3):144–9. [PubMed: 11321599]
28. Embree MC, Chen M, Pylawka S, Kong D, Iwaoka GM, Kalajzic I, Yao H, Shi C, Sun D, Sheu TJ, Koslovsky DA, Koch A, Mao JJ. Exploiting endogenous fibrocartilage stem cells to regenerate cartilage and repair joint injury. Nat Commun. 2016; 7:13073. [PubMed: 27721375]
29. Koyama E, Ochiai T, Rountree RB, Kingsley DM, Enomoto-Iwamoto M, Iwamoto M, Pacifici M. Synovial joint formation during mouse limb skeletogenesis: roles of Indian hedgehog signaling. Ann N Y Acad Sci. 2007; 1116:100–12. [PubMed: 18083924]
30. St-Jacques B, Hammerschmidt M, McMahon AP. Indian hedgehog signaling regulates proliferation and differentiation of chondrocytes and is essential for bone formation. Genes Dev. 1999; 13(16): 2072–86. [PubMed: 10465785]
31. Maeda Y, Nakamura E, Nguyen MT, Suva LJ, Swain FL, Razzaque MS, Mackem S, Lanske B. Indian Hedgehog produced by postnatal chondrocytes is essential for maintaining a growth plate and trabecular bone. Proc Natl Acad Sci U S A. 2007; 104(15):6382–7. [PubMed: 17409191]
32. Kinumatsu T, Shibukawa Y, Yasuda T, Nagayama M, Yamada S, Serra R, Pacifici M, Koyama E. TMJ development and growth require primary cilia function. J Dent Res. 2011; 90(8):988–94. [PubMed: 21566205]
33. Ochiai T, Shibukawa Y, Nagayama M, Mundy C, Yasuda T, Okabe T, Shimono K, Kanyama M, Hasegawa H, Maeda Y, Lanske B, Pacifici M, Koyama E. Indian hedgehog roles in post-natal TMJ development and organization. J Dent Res. 2010; 89(4):349–54. [PubMed: 20200412]
34. Ishizuka Y, Shibukawa Y, Nagayama M, Decker R, Kinumatsu T, Saito A, Pacifici M, Koyama E. TMJ degeneration in SAMP8 mice is accompanied by deranged Ihh signaling. J Dent Res. 2014; 93(3):281–7. [PubMed: 24453178]

35. Purcell P, Joo BW, Hu JK, Tran PV, Calicchio ML, O'Connell DJ, Maas RL, Tabin CJ. Temporomandibular joint formation requires two distinct hedgehog-dependent steps. Proc Natl Acad Sci U S A. 2009; 106(43):18297–302. [PubMed: 19815519]
36. Henry SP, Jang CW, Deng JM, Zhang Z, Behringer RR, de Crombrugghe B. Generation of aggrecan-CreERT2 knockin mice for inducible Cre activity in adult cartilage. Genesis. 2009; 47(12):805–14. [PubMed: 19830818]
37. Sinha S, Mundy C, Bechtold T, Sgariglia F, Ibrahim MM, Billings PC, Carroll K, Koyama E, Jones KB, Pacifici M. Unsuspected osteochondroma-like outgrowths in the cranial base of Hereditary Multiple Exostoses patients and modeling and treatment with a BMP antagonist in mice. PLoS Genet. 2017; 13(4):e1006742. [PubMed: 28445472]
38. Bai CB, Auerbach W, Lee JS, Stephen D, Joyner AL. Gli2, but not Gli1, is required for initial Shh signaling and ectopic activation of the Shh pathway. Development. 2002; 129(20):4753–61. [PubMed: 12361967]
39. Farnum CE, Wilsman NJ. Determination of proliferative characteristics of growth plate chondrocytes by labeling with bromodeoxyuridine. Calcif Tissue Int. 1993; 52(2):110–9. [PubMed: 8443686]
40. He Y, Zhang M, Huang AY, Cui Y, Bai D, Warman ML. Confocal imaging of mouse mandibular condyle cartilage. Sci Rep. 2017; 7:43848. [PubMed: 28266618]
41. Lanske B, Karaplis AC, Lee K, Luz A, Vortkamp A, Pirro A, Karperien M, Defize LH, Ho C, Mulligan RC, Abou-Samra AB, Juppner H, Segre GV, Kronenberg HM. PTH/PTHrP receptor in early development and Indian hedgehog-regulated bone growth. Science. 1996; 273(5275):663–6. [PubMed: 8662561]
42. Vortkamp A, Lee K, Lanske B, Segre GV, Kronenberg HM, Tabin CJ. Regulation of rate of cartilage differentiation by Indian hedgehog and PTH-related protein. Science. 1996; 273(5275): 613–22. [PubMed: 8662546]
43. Kobayashi T, Soegiarto DW, Yang Y, Lanske B, Schipani E, McMahon AP, Kronenberg HM. Indian hedgehog stimulates periarticular chondrocyte differentiation to regulate growth plate length independently of PTHrP. J Clin Invest. 2005; 115(7):1734–42. [PubMed: 15951842]
44. Mak KK, Kronenberg HM, Chuang PT, Mackem S, Yang Y. Indian hedgehog signals independently of PTHrP to promote chondrocyte hypertrophy. Development. 2008; 135(11):1947–56. [PubMed: 18434416]
45. Porter JA, von Kessler DP, Ekker SC, Young KE, Lee JJ, Moses K, Beachy PA. The product of hedgehog autoproteolytic cleavage active in local and long-range signalling. Nature. 1995; 374(6520):363–6. [PubMed: 7885476]
46. Zeng X, Goetz JA, Suber LM, Scott WJ Jr, Schreiner CM, Robbins DJ. A freely diffusible form of Sonic hedgehog mediates long-range signalling. Nature. 2001; 411(6838):716–20. [PubMed: 11395778]
47. Koziel L, Kunath M, Kelly OG, Vortkamp A. Ext1-dependent heparan sulfate regulates the range of Ihh signaling during endochondral ossification. Dev Cell. 2004; 6(6):801–13. [PubMed: 15177029]
48. Chan JA, Balasubramanian S, Witt RM, Nazemi KJ, Choi Y, Pazyra-Murphy MF, Walsh CO, Thompson M, Segal RA. Proteoglycan interactions with Sonic Hedgehog specify mitogenic responses. Nat Neurosci. 2009; 12(4):409–17. [PubMed: 19287388]
49. Billings PC, Pacifici M. Interactions of signaling proteins, growth factors and other proteins with heparan sulfate: mechanisms and mysteries. Connect Tissue Res. 2015; 56(4):272–80. [PubMed: 26076122]
50. Shimo T, Gentili C, Iwamoto M, Wu C, Koyama E, Pacifici M. Indian hedgehog and syndecans-3 coregulate chondrocyte proliferation and function during chick limb skeletogenesis. Dev Dyn. 2004; 229(3):607–17. [PubMed: 14991716]
51. Koyama E, Young B, Nagayama M, Shibukawa Y, Enomoto-Iwamoto M, Iwamoto M, Maeda Y, Lanske B, Song B, Serra R, Pacifici M. Conditional Kif3a ablation causes abnormal hedgehog signaling topography, growth plate dysfunction, and excessive bone and cartilage formation during mouse skeletogenesis. Development. 2007; 134(11):2159–69. [PubMed: 17507416]

## Highlights

- Development of polymorphic/progenitor layer and structure of condylar articular cartilage is clarified during postnatal TMJ development.
- Chondroprogenitors and their fate are clarified in postnatal condylar articular cartilage.
- We evaluate gene recombination in postnatal TMJs using *Aggrecan (Agc)-CreER;R26-tdTomato* reporter mice.
- The role of hedgehog signaling is clarified in postnatal TMJs using compound *Agc-CreER;Ihh f/f;Gli1-nLacZ* mice
- Ablation of Ihh signaling in postnatal *Agc-CreER;Ihh f/f* mice disrupts chondroprogenitor cell function, resulting in degenerative changes in cartilage and suboptimal subchondral bone formation.
- Hh signaling promotes chondrogenesis and chondrocyte maturation in condylar apical cell culture.

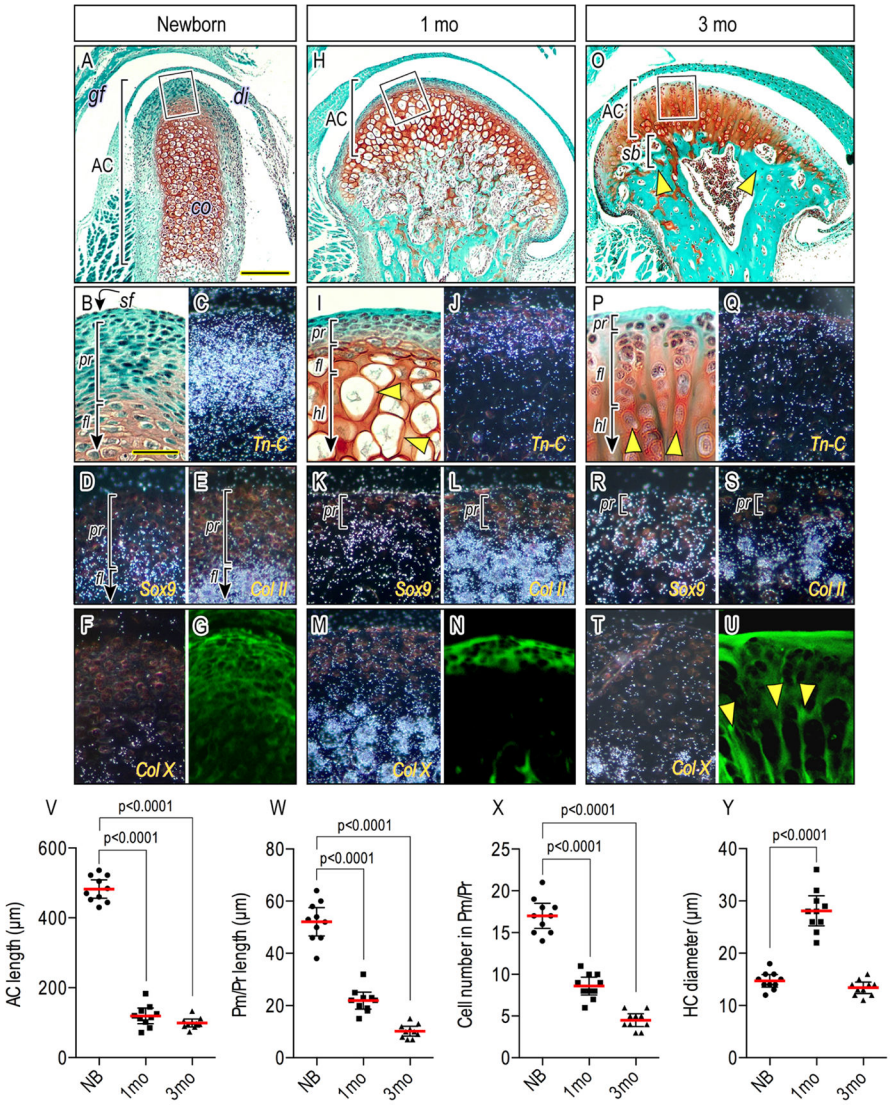


**Figure 1.**

Condylar articular cartilage development, zonal organization, cellularity and matrix configuration over age. Mid-frontal portions of TMJs from newborn (A–G), 1-month (H–N) and 3-month (O–U)-old wild-type mice were analyzed by Safranin-O/fast-green staining (A, B, H, I, O, P), i*n situ* hybridization (C–F, J–M, Q–T), and a confocal microspopy-detectable cartilage matrix (G, N, U). Boxed-area of condylar apical end (A, H, O) was magnified in (B, I, P). Brackets demarcate polymorphic/progenitor layer (*pr*), flattened chondrocyte layer (*fl*), hypertrophic chondrocyte layer (*hl*) and subchondral bone plate (*sb*). *In situ* hybridization with isotope-labeled riboprobes for *Tn-C* (C, J, Q), *Sox9* (D, K, R), *Col II* (E, L, S) and *Col X* (F, M, T) expression. (V): Articular cartilage (AC) length, (W): polymorphic/progenitor (Pm/Pr) length, (X): cell number in Pm/Pr, and (Y) hypertrophic chondrocyte diameter of distinct TMJs from wild-type mice at age of newborn, 1 month and 3 months were analyzed. Areas were selected from 3–5 mid-frontal sections per sample and 10 TMJs were analyzed ($n$=10/each group, $p$ values are indicated in the scatter plots). The

dots represent the mean data of 10 TMJ samples ($n$=10). The long red horizontal bar represents the mean value and the short horizontal bars represent 95% confidence intervals. Scale bars: 90 μm in A for A, H, O; 25 μm in B for B–G, I–N, P–U. *gf, glenoid fossa; dc, disc; cd, condyle, lp, lateral pterygoid muscle, AC, articular cartilage, sf, superficial layer; pr, polymorphic/progenitor layer; fl, flattened chondrocyte layer; hl, hypertrophic layer; sb, subchondral bone plate.*

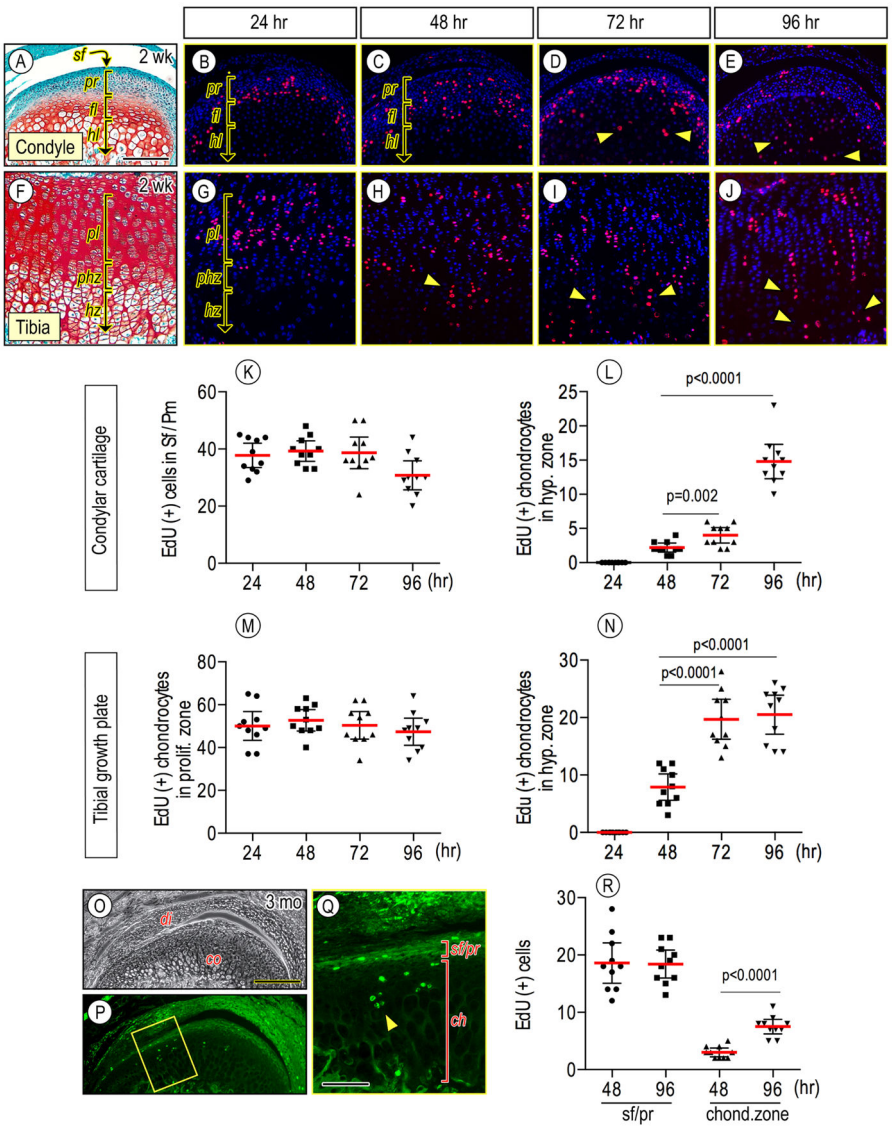


**Figure 2.**

Edu leveling and tracing analyses in condylar articular cartilage and tibial growth plate in juvenile and adult mice. Wild-type mice were injected with EdU at age of 2 weeks (A–J) or 3 months (O–Q) and EdU-positive cells were analyzed in condyles (A–E, K–L, O–R) and tibial growth plates (F–J, M–N) from the same mouse after 24 hr (B, G), 48 hr (C, H), 72 hr (D, I) and 96 hr (E, J, O–Q) from the first EdU injection. Note that fewer EdU-labeled chondroprogenitors were observed (2R), but were still detectable at the superficial/progenitor layers (*sf/pr*) of the condylar apical end and in the underlying chondrocyte zones (*ch*) by 96 hr (P, Q). EdU-labled cells were detected by RFP (B–E, G–J) and by GFP (P–Q). Relative area of superficial (*sf*) and polymorphic/progenitor (*pr*) layers and flattened (*fl*) and hypertrophic (*hl*) chondrocyte layers in condylar cartilage and proliferating (*pl*), prehypertrophic (*phz*) and hypertrophic (*hz*) zones of tibial growth plate were evaluated by histological morphometry. EdU-positive cells in condylar cartilage or tibial growth plates (approximately 250 × 250 μm$^2$) were counted in 3–5 mid-frontal sections per sample. Ten

TMJs and knee joints were analyzed ($n$=10/each group, $p$ values are indicated in the scatter plots). The long red horizontal bar represents the mean value and the short horizontal bars represent 95% confidence intervals (K–L, R). Scale bars: 55 μm in A for A–J; 190 μm in O for O–P; 75 μm in Q. *sf, superficial layer; pr, polymorphic/progenitor layer; sf/pr, superficial-polymorphic/progenitor layer; fl, flattened chondrocyte layer; hl, hypertrophic chondrocyte layer; ch, chondrocyte zone; pl, proliferating zone, phz, prehypertrophic zone; hz, hypertrophic zone.*

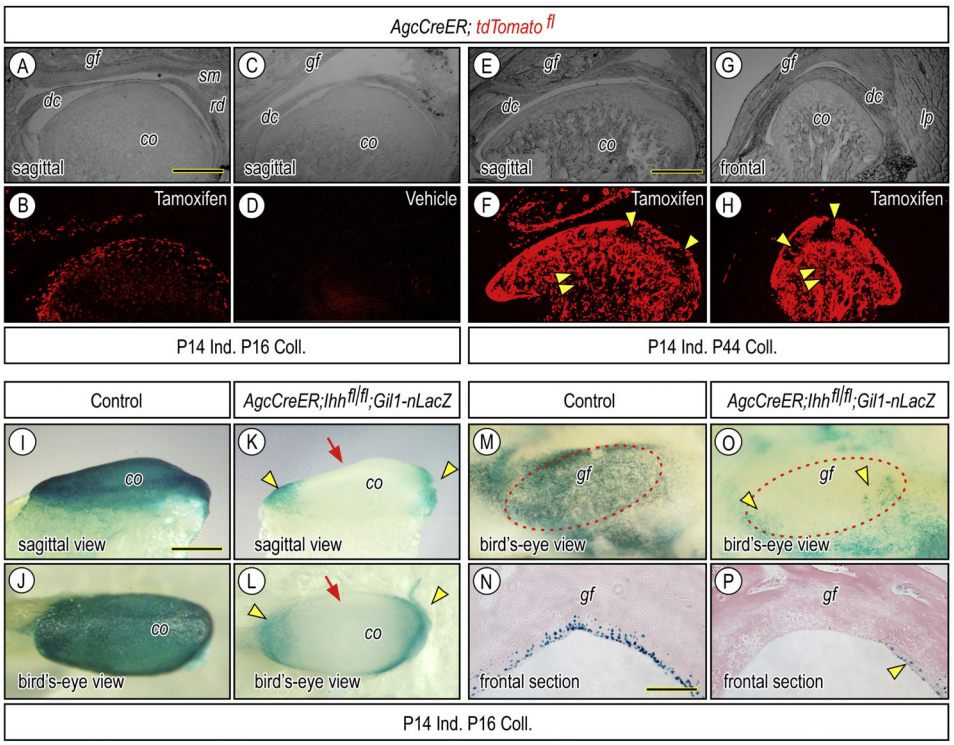


**Figure 3.**

Clarification of Cre recombinase activity and inactivation of hedgehog signal in postnatal TMJs of *Agc-CreER; Ihh* $^{f/f}$*;Gli1-nLacZ*. Bright field (A, C, E, G) and corresponding fluorescence (B, D, F, H) images of parasagittal (A–F) and frontal (G–H) sections of TMJs from which *Agc-CreER-tdTomato* $^{fl}$ mice had been administrated tamoxifen once (A, B, E–H) or vehicle (C, D) at P14 and were sacrificed at P16 (A–D) or at P44 (E–H). Fluorescence images (B, F, H) show that reporter activity is detected in superficial cells, progenitors and chondrocytes of the articular cartilage of the glenoid fossa and condyle, but is absent from the articular disc (*dc*), retrodiscal tissue (*rd*) and synovial membrane (*sm*). Strong reporter activity is also detected in marrow cells (F, H: arrowheads). Whole mount LacZ staining (I–M, O) and frontal section (N, P) of condyles (I–L) and glenoid fossa (M–P) obtained from P16 -*Agc-CreER; Ihh* $^{f/f}$*;Gli1-nLacZ* or control P16-*Agc-CreER; Ihh* $^{f/f}$*;Gli1-nLacZ* that had been injected with tamoxifen (I–P) at P14. LacZ-positive cells resided at the anterior and posterior ends of the condylar articular cartilage (K, L, arrowheads) and at the medial, lateral, anterior and posterior edges of the fossa (O, P, arrowheads). Scale bars: 160 μm in A for A–D; 220 μm in E for E–H; 200 μm in I for I–M, O; 130 μm in N for N, P. *gf, glenoid fossa; dc, articular disc; cd, mandibular condyle, lp, lateral pterygoid muscle.*

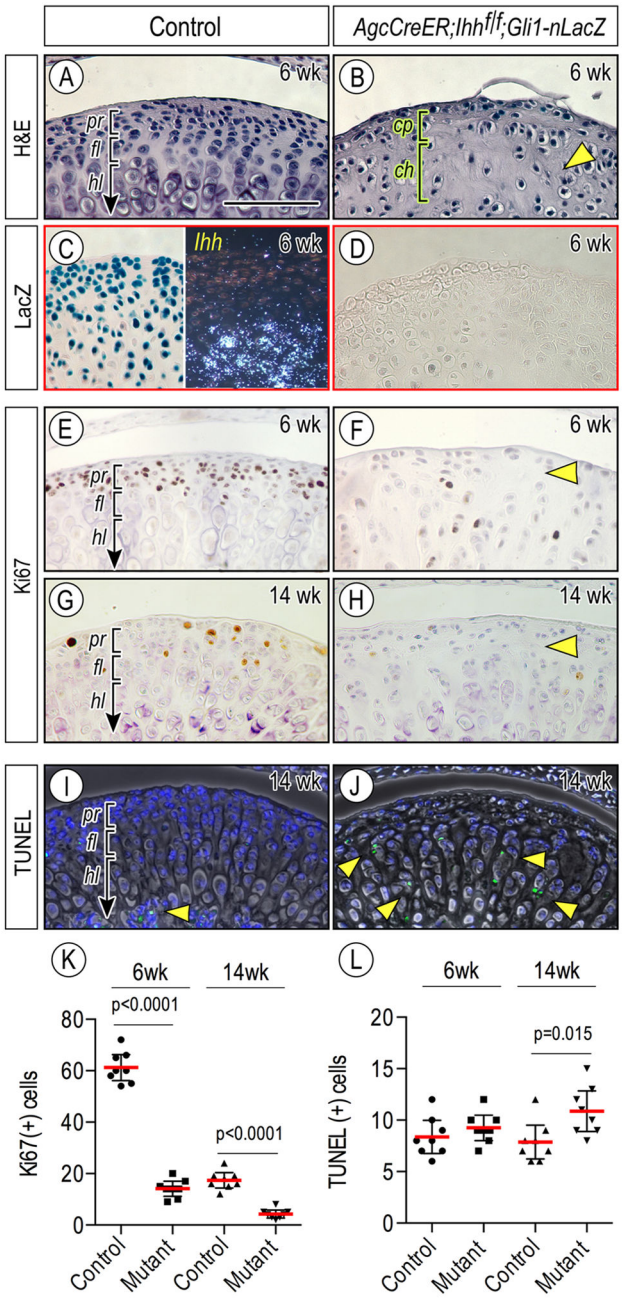


**Figure 4.**

Condylar articular cartilage zonal organization and cellularity are abnormal in *Agc-CreER; Ihh f/f;Gli1-nLacZ* mice over time. Mid-frontal portion of TMJs from 6-week (A–F) and 14-week (G–J) of control (A, C, E, G, I) and *Agr-CreER;Ihh f/f* (B, D, F, H, J) mice were analyzed by hematoxylin and eosin staining (A, B), LacZ staining (C, left panel; D), Ki67 staining (E–H), in situ hybridization of *Ihh* gene expression (C, right panel) and TUNEL staining (I, J). Ki67-positive cells (E–H) in the polymorphic/progenitor layer or TUNEL-positive cells (I, J) in the entire area of condylar cartilage in mid-sagittal serial sections randomly selected were counted and present as absolute numbers, and eight TMJs/group

were analyzed ($n$=8/group, $p$ values are indicated in the scatter plots). Statistical analysis of K67-expressing (K) or TUNEL-positive (L) cells. The long red horizontal bar represents the mean value and the short horizontal bars represent 95% confidence intervals. Scale bars: 75 μm in A for A–J. *pr, polymorphic/progenitor layer; fl, flattened chondrocyte layer; hl, hypertrophic chondrocyte layer.*

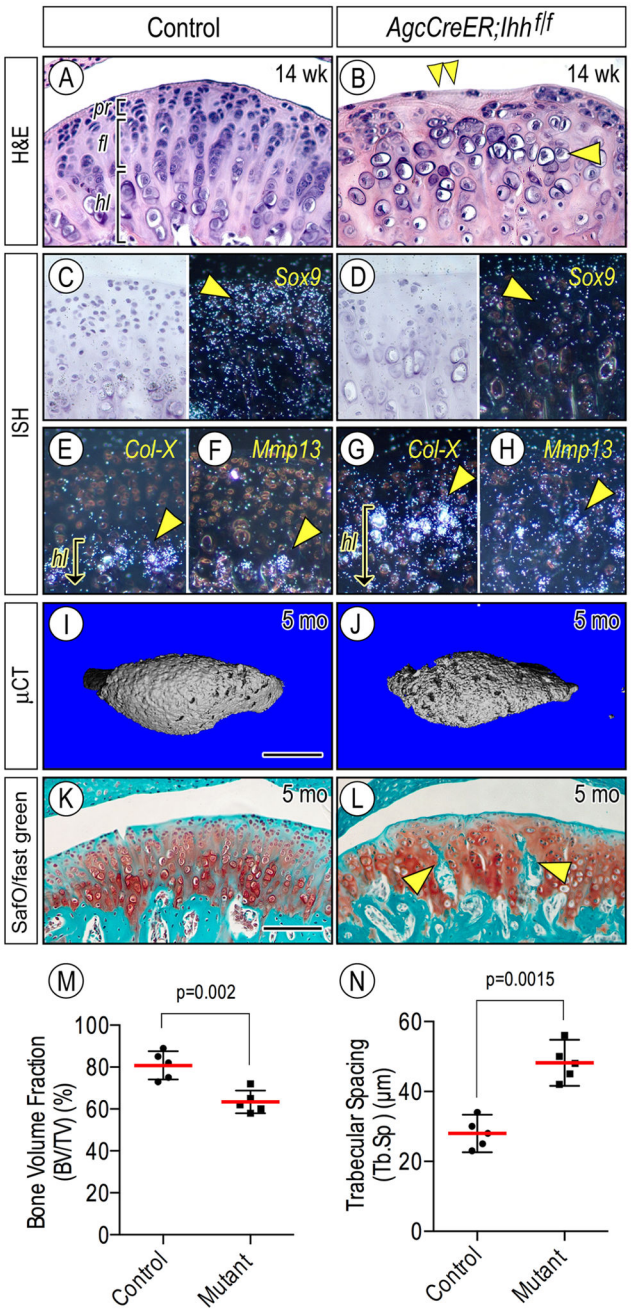


**Figure 5.**

Defective condylar articular cartilage and subchondral bone in *Agr-CreER; Ihh* $^{f/f}$ mice over time. TMJs from 14-week (A–H) and 5-month (K–L) of control (A, C, E, F, I, K) and *Agr-CreER;Ihh* $^{f/f}$ (B, D, G, H, J, L) mice were analyzed by hematoxylin and eosin staining (A, B), *in situ* hybridization (C–H), μCT (I, J), and Safranin-O/fast green staining (K, L). *In situ* hybridization with isotope-labeled riboprobes for *Tn-C* (C, D), *Col-X* (E, G), and *Mmp13* (F, H) expression. Note that *Col-X/Mmp13*-expressing hypertrophic chondrocytes in mutant condyles reside closer to the condylar surface compared to controls (E–H, arrowhead, respectively). Quantification of bone volume fraction (TB/TV) (M) and travecular spacing

(Tb.Sp) (N) of condylar subchondral bone plate by μCT. Five TMJs/group were analyzed ($n$=5/group, $p$ values are indicated in the scatter plots) and data plots, average and 95% confidence intervals are presented. Scale bars: 75 μm in A for A–H; 220 μm in I for I–J; 125 μm in K for K–L. *pr, polymorphic/progenitor layer; fl, flattened chondrocyte layer; hl, hypertrophic chondrocyte layer.*

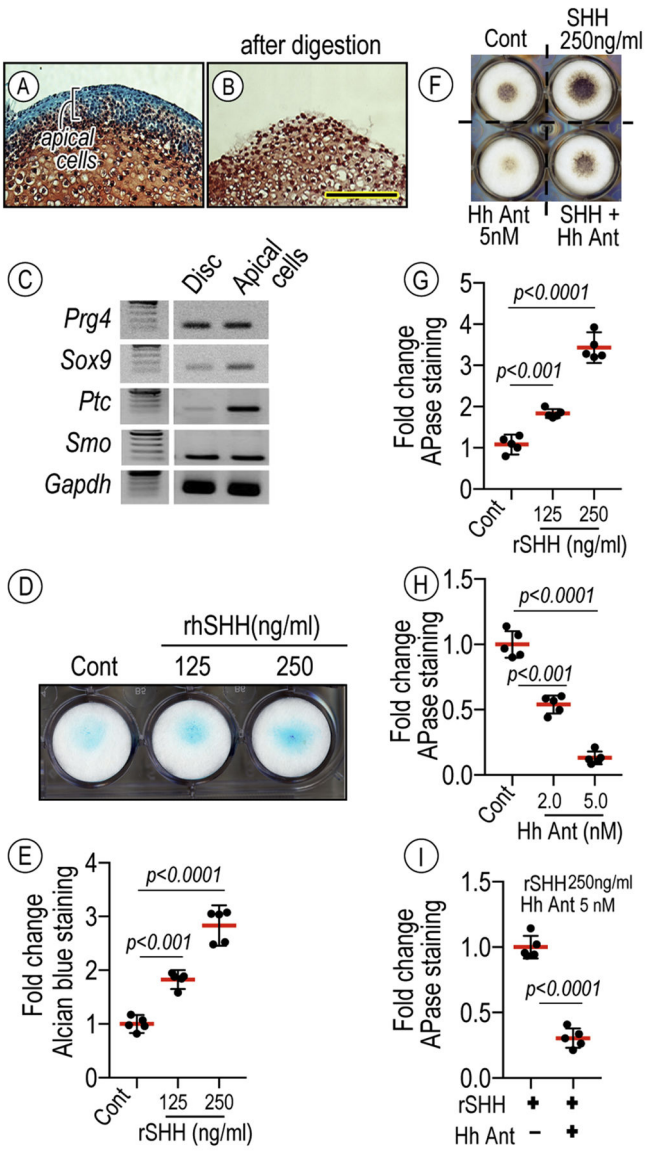


**Figure 6.**

Hh-induced stimulatory effect on chondrogeneis and chondrocyte maturation by primary condylar apical cells.

Condylar cartilage isolated from P7 mice before (A) and after (B) a sequential digestion (i.e. 0.25% trypsin followed by 0.1U collagenase for 5 min per each digestion) were sectioned and stained with Safranin-O/fast green, revealing the isolation of apical cells of the condyles. Semi-quantitative PCR analysis revealing characteristic gene expression including superficial and chondrogenic markers such as *Proteoglycan 4* (*Prg4*) and *Sox9* as well as Hh receptors, *Patched 1* (*Ptc*) and *Smo*, thus distinguishing the expression prolife of apical cells from articular discs. Condylar apical cells cultured in a high-density micromass culture (D) on 24-well plates in the absence or presence of rhSHH protein (125 and 250 ng/ml), Hh Antag (2 and 5 nM), a combination of rhSHH and Hh Antag for 7 days, fixed, and processed for Alcian blue staining (D) or APase activity (F). Statistical analyses evaluated by

integrated density of Alcian blue- (E) or APase- (G–I) stained cultures measured by ImageJ (*n=5, p* values are indicated in the scatter plots). The long red horizontal bar represents the mean value and the short horizontal bars represent 95% confidence intervals. Scale bar: 75 μm in B for A–B.

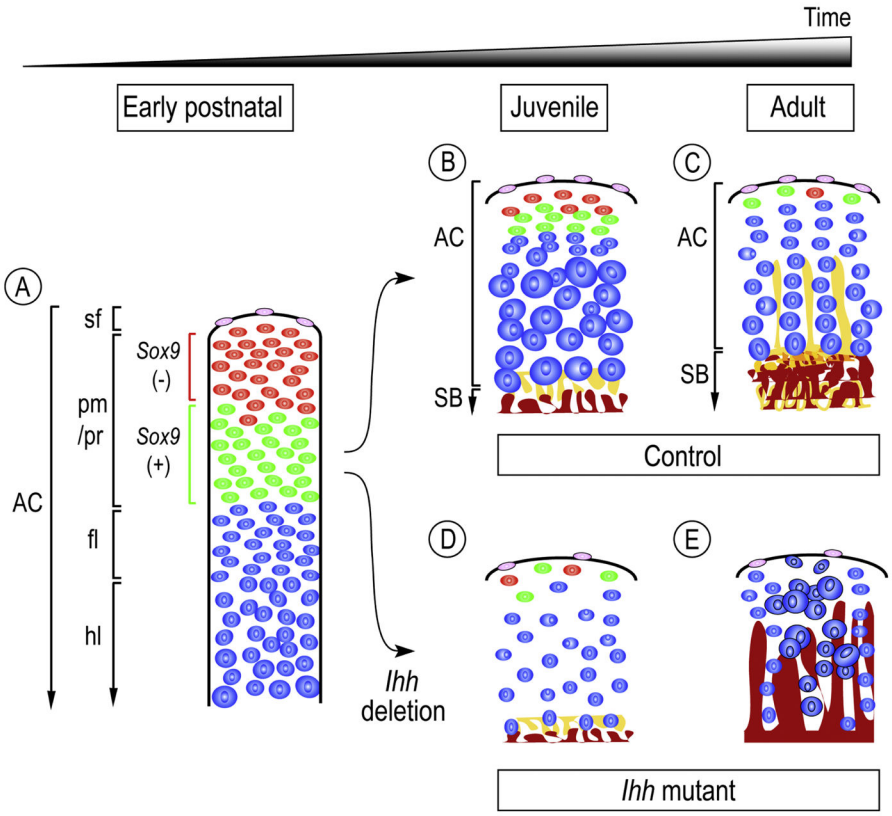


**Figure 7.**

Model of condylar articular cartilage development during postnatal stages and the roles of Ihh signaling in the processes. Starting at neonatal stages and proceeding into adult, condylar articular cartilage (AC) would progressively acquire its functional organization and structure that demarcate: superficial layer (*sf*), polymorphic/progenitor layer (pm/*pr*), flattened immature chondrocyte layer (*fl*), hypertrophic chondrocyte layer (*hl*), which is supported by subchondral bone plate (SB) (A). The progenitor layer is composed of *Tn-C*(+)*;Sox-9*(−) (painted red) and *Tn-C*(+)*;Sox-9*(+) (painted green) cells (A). *Tn-C*(+)*;Sox-9*(−) cells become less and no longer, if any, reside in the adult condylar cartilage (B, C). Longitudinal growth and lateral expansion of the condylar articular cartilage at juvenile and young adult stages would be driven by proliferation of chondroprogenitor cells followed by chondrogenesis, and by chondrocyte volume increase, particularly at juvenile stages (B). *Tn-C*(+)*;Sox-9*(−) cells would serve as a pool of chondroprogenitors during postnatal development of condylar articular cartilage. The characteristic chondrocyte column formation would become apparent along with the development of subchondral bone plate (pained brown) and vertical septa of cartilage matrix (pained yellow) (C). In the absence of *Ihh* signaling at juvenile stages (*Agc-CreER;Ihh* $^{f/f}$), condylar articular cartilage would display: 1) decreased superficial and *Tn-C*(+)*;Sox-9*(−) (painted red) and *Tn-C*(+)*;Sox-9*(+) (painted green) cells (D), 2) decreased chondrocytes and loss of chondrocyte topographical arrangement (D, E), 3) ectopic chondrocyte hypertrophy (E), and 4) deranged articular

subchondral bone plate (E). Note that the model focuses on the central region of the condylar articular cartilage.